ISSN 1027-5495. Functional Materials, 25, No.3 (2018), p. 525-533.
doi:https://doi.org/10.15407/fm25.03.525

Kinetics of crystals growth under electron-beam crystallization of amorphous films of hafnium dioxide

A.G.Bagmut, I.A.Bagmut

NTU "KhPI", 2 Kyrpychova Str., 61002 Kharkiv, Ukraine

Received February 21, 2018

Amorphous films of HfO_2 are prepared by laser ablation of Hf target in an oxygen atmosphere. Its crystallization was performed under the electron beam impact in a column of electron microscope. Formation and growth of HfO_2 crystals are investigated "in situ". The transformation kinetic curves are plotted on the basis of a frame-by-frame analysis of the video recorded flick during the film crystallization. According to the structural and morphological features, the phase transformation corresponds to the dendrite polymorph crystallization and can be either single-stage or two-stage in nature. In the latter case, the size-phase effect takes place, consisting in the fact, that when the crystal of orthorhombic modification of HfO_2 reaches a critical size (~0.2 μm), it splits into domains with orthorhombic and monoclinic crystal lattices. The kinetic parameters of the crystallization are determined and it is shown, that the quadratic dependence of the fraction of the crystalline phase on time takes place. The average value of the relative length for the dendrite polymorphic crystallization is about 3075. The phase transition from the amorphous state to the crystalline one is accompanied by increasing of the relative density of matter of the film by about 2.5 %. The crystallized film consists predominantly of dendrites of the monoclinic modification of HfO_2.

Keywords: kinetic of phase transformation, in situ TEM, electron irradiation, dendrites, hafnium dioxide, amorphous films.

Аморфные пленки HfO_2 получены лазерной абляцией мишени Hf в атмосфере кислорода. Их кристаллизацию осуществляли воздействием электронного луча в колонне электронного микроскопа. Образование и рост кристаллов HfO_2 исследован "на месте". Кинетические кривые превращения построены на основе покадрового анализа видеофильма процесса кристаллизации пленки. По структурно-морфологическим признакам фазовое превращение соответствует дендритной полиморфной кристаллизации и может носить как одностадийный, так и двустадийный характер. В последнем случае имеет место размерно-фазовый эффект, состоящий в том, что когда размер кристалла орторомбической модификации HfO_2 превышает критическую величину (~0.2 мкм), то он расщепляется на домены, которые имеют как орторомбическую, так и моноклинную кристаллическую решетку. Определены кинетические параметры кристаллизации и показано, что имеет место квадратичная зависимость доли кристаллической фазы от времени. Среднее значение относительной длины при дендритной полиморфной кристаллизации составляет ~ 3075. Фазовое превращение из аморфного в кристаллическое состояние сопровождается увеличением относительной плотности вещества пленки на ~ 2.5 %. После полной кристаллизации пленка состоит преимущественно из дендритов моноклинной модификации HfO_2.

Кінетика росту кристалів під час електронно-променевої кристалізації аморфних плівок діоксиду гафнію. *О.Г.Багмут, І.О.Багмут.*

Аморфні плівки HfO_2 отримано лазерною абляцією мішені Hf в атмосфері кисню. Їх кристалізацію здійснювали впливом електронного променя у колоні електронного мікроскопа. Формування і зростання кристалів HfO_2 досліджено "на місці". Кінетичні криві перетворення побудовано на основі покадрового аналізу відеофільму процесу кристалізації плівки. За структурно-морфологічними ознаками фазове перетворення відповідає дендритній поліморфній кристалізації і може носити як одностадійний, так і двостадійний характер. В останньому випадку має місце розмірно-фазовий ефект, який полягає у тому, що коли розмір кристала орторомбічної модифікації HfO_2 перевищує критичну величину (~ 0.2 мкм), то він розщеплюється на домени, які мають як орторомбічну, так і моноклінну кришталеву гратку. Визначено кінетичні параметри кристалізації і показано, що має місце квадратична залежність частки кристалічної фази від часу. Середнє значення відносної довжини при дендритній поліморфній кристалізації складає ~ 3075. Фазове перетворення з аморфного стану у кристалічний стан супроводжується збільшенням відносної щільності речовини плівки на ~ 2.5 %. Після повної кристалізації плівка складається переважно з дендритів моноклінної модифікації HfO_2.

1. Introduction

Hafnium dioxide (HfO_2) in thin film state attracts significant interest owing to their high values of its dielectric constant, refractive index, neutron absorption cross section, and also thermal stability (melting point ~ 2800°C) [1]. Besides this amorphous gate insulators are more preferred than the crystalline one since they can effectively reduce the problems, arising from the crystal orientation, grain boundary, and the lattice mismatch at the interfaces [2]. Amorphous films of HfO_2 can be prepared with different methods: atomic layer deposition [3], chemical vapor deposition [4], ion-plasma sputtering of HfO_2 targets [5] and others.

Method of pulsed laser deposition (PLD) also finds a wide application in production of the films and coatings of HfO_2. Laser ablation of hafnium dioxide leads to formation on the substrate of a layer, consisting of tetragonal and cubic HfO_2 nanoparticles, having a spherical shape and sizes from 10 to 100 nm [6]. Method of pulsed laser evaporation of hafnium target in an oxygen atmosphere leads to formation on the substrate of amorphous layer of HfO_2 at room temperature [7, 8].

Electron-beam crystallization of the amorphous HfO_2 is accompanied by formation of dendrites crystals. The dendrites are formed both from the embryos of HfO_2 monoclinic modification, and from the embryos of HfO_2 orthorhombic modification. In the latter case, the dimension-phase effect takes place [8]. It manifests itself in the fact, that when the HfO_2 crystal of orthorhombic modification reaches a critical size (~ 0.2 μm), the domains of the monoclinic modification of HfO_2 are formed in it. Therefore, at the final stage of the film crystallization, the dominant component is the monoclinic phase represented by the dendrites of HfO_2 crystals.

"In-situ" transmitting electron microscopy is an effective method for studying the structural, morphological and kinetic features of the phase transition from the amorphous to crystalline state in thin films [9, 10]. This method makes it possible to determine both the structural and morphological changes and the numerical values of the relative change in density and the kinetic parameters of the substance crystallization. Based on the results of the electron microscopic investigations and analysis of the data available in the literature, classification of the types of crystallization of amorphous films in accordance with their structural and morphological features was proposed in [11, 12]. According to this classification, the following types of crystallization modes are distinguished: the layer (LPC), island (IPC), and dendrite (DPC) polymorphic crystallizations, as well as the fluid-phase crystallization (FPC) accompanied by the medium separation.

Quantitative data on morphology and kinetics of crystallization of the films are important for predicting of the stability and properties of the amorphous components of electronic devices. Such data are not available for amorphous HfO_2. Therefore, the aim of this work was to obtain the amorphous HfO_2 films by PLD method, to study their structure, morphology and kinetics of the electron-beam crystallization.

2. Experimental

Films of HfO_2 were prepared by PLD technique in oxygen atmosphere at pressure of ~ 0.13 Pa. Sputtering of a high-purity hafnium target was carried out with the use of pulsed laser radiation from an LTI-PCh-5 laser operating in the Q-switched mode. The laser target erosion products were deposited on KCl (001) substrates at the room temperature. Thickness of the films varied in the range from 25 to 30 nm. Details of the pulsed laser deposition technique were described in [13, 14]. Crystallization of the film was initiated by electron beam irradiation in a column of transmission electron microscope at the beam current of ~ 20 μA. The crystallization rate was controlled by varying the density j of the electron current through the sample, which was varied in the range from 1.1 to 6.5 A·mm^{-2} depending on the electron beam focusing.

Phase and structural analysis was performed using the electron diffraction and transmission electron microscopy methods. The film crystallization process was registered in the video recording mode at a frame rate of 30 s^{-1} [15, 16]. Data on the kinetics of the crystallization process were obtained from the analysis of individual frames of the video recorded "in situ" at a fixed tangential crystal growth rate ν (specified by the electron current density j), which is determined by the following relationship:

$$\nu = \frac{\Delta D}{\Delta t}, \qquad (1)$$

where ΔD is the increment in the average value of diameter D of HfO_2 microcrystal during a time period Δt between the two video frames corresponding to the moments of the recording t and $t + \Delta t$. The crystals size was determined from the contrast of the electron microscopy image, because it was different from the contrast of the electron microscopy image of the amorphous matrix.

The relative change γ in density ρ of the material of the film after its crystallization [10] was determined according to (2):

$$\gamma = \frac{\rho_c - \rho_a}{\rho_a} = \left(\frac{L_a}{L_c}\right)^3 - 1, \qquad (2)$$

where ρ_c and ρ_a are the material densities in the crystalline and amorphous states, respectively, and L_a and L_c are the distances between fixed marks in the same region of the images before and after films crystallization. The marks were the solidified micro droplets of the melt of Hf (the spraying effect).

3. Results and discussion

The PLD of Hf in oxygen atmosphere resulted in formation of the amorphous HfO_2 films on substrate at the room temperature. Electron-beam crystallization of the film leads to formation of HfO_2 crystals with different structure and morphology.

Fig. 1a shows an electron microscopic image, illustrating the beginning of crystallization of the amorphous phase. Crystal 1 has pronounced dendrite morphology, which manifests itself in the presence of branches of the first and second order. Studies have shown that such crystals have a monoclinic crystal lattice and during their growth its structure and dendrite morphology do not change. Crystal 2 has a disk-like shape. The selected area electron diffraction (SAED) pattern of this crystal is shown in Fig. 1b. The results obtained by interpreting of this SAED pattern show that this is an orthorhombic modification of hafnium dioxide. Crystals with a number 2 in Fig. 1a and 1c have the orthorhombic lattice. In the process of its growth, when their diameter D exceeds the critical value D^*, the polymorphic transformation occurs to the monoclinic modification of HfO_2. It is accompanied by the formation of domains with the monoclinic crystal lattice within the disc-shaped crystal of HfO_2.

Fig. 1c shows a bright-field electron microscopic image of the disc-shaped crystals (numbered as 2), whose diameter is less than D^*. The crystal with a dark contrast is in a reflective position. The crystallites, numbered as 3, have diameter $D > D^*$. They consist of domains of the orthorhombic and monoclinic modifications of HfO_2.

The SAED pattern of one of these crystallites, containing reflexes of both the original orthorhombic modification ("or" indices) and the new monoclinic modification ("m" indices), is shown in Fig. 1d. The inset in the right upper corner of Fig. 1c corresponds to the dark-field image of this crystal in the light of the reflection $(\bar{1}12)_{or}$. The domains of orthorhombic modification have $[\bar{1}1\bar{1}]_{or}$ zone axis, and domains of the monoclinic modification have $[1\bar{1}0]_m$ zone axis. In this case, between the domains of both types, the orientation relation is fulfilled:

$$(30\bar{3})_{or}[\bar{1}1\bar{1}]_{or} /\!/ (\bar{2}2\bar{3})_m[1\bar{1}0]_m. \qquad (3)$$

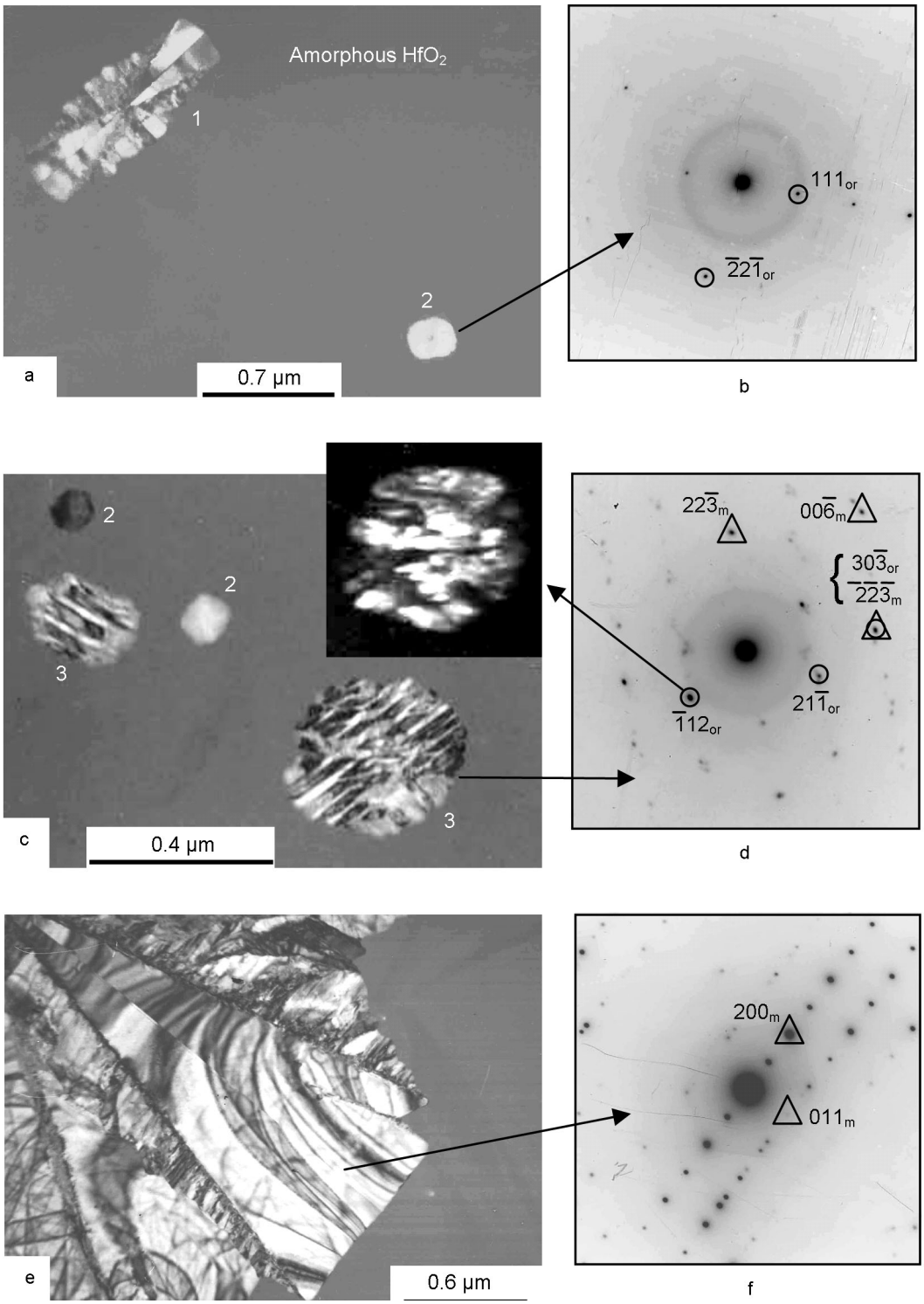

Fig. 1. "In situ" electron-beam crystallization of amorphous film of HfO_2. (a) Electron microscope images of dendrite (*1*) and disc-like (*2*) crystals of HfO_2. (b) The SAED pattern of the disc-like crystal (*2*), containing reflexes of orthorhombic modification of HfO_2. (c) Electron microscope images of disc-like crystals of HfO_2 with size smaller than the critical (*2*) and crystallites with size larger than the critical (*3*). The inset in the right upper corner corresponds to dark-field image of the crystallite (*3*) in the light of reflection $(\bar{1}12)_{or.}$ (d). The SAED pattern of the crystallite (*3*), containing reflexes of orthorhombic and of monoclinic modification of HfO_2. (e) Dendrite branches and SAED pattern of the first-order dendrite branch (f). Contrast on the SAED patterns is inverted.

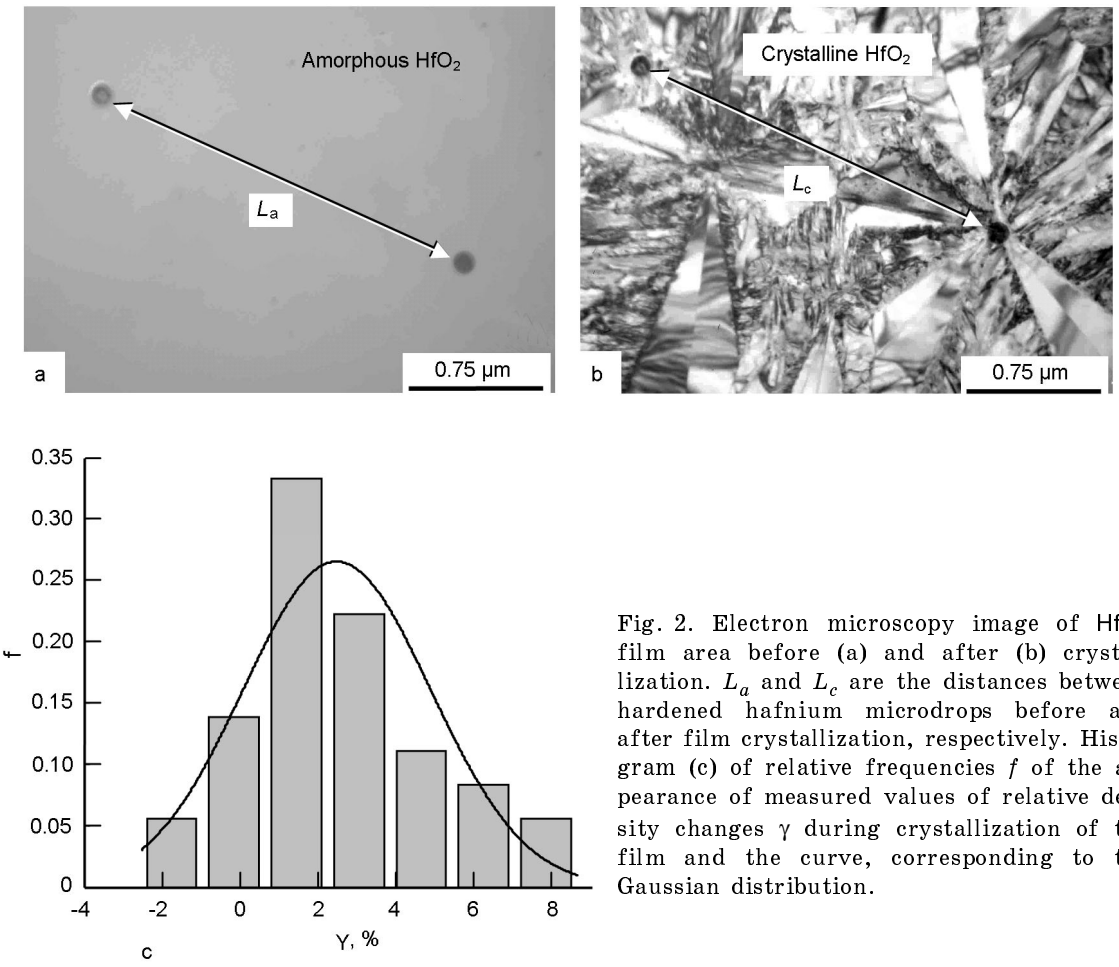

Fig. 2. Electron microscopy image of HfO_2 film area before (a) and after (b) crystallization. L_a and L_c are the distances between hardened hafnium microdrops before and after film crystallization, respectively. Histogram (c) of relative frequencies f of the appearance of measured values of relative density changes γ during crystallization of the film and the curve, corresponding to the Gaussian distribution.

As crystallites grow, they acquire the dendrite morphology with branches of the first, second and higher orders, which have monoclinic lattice of HfO_2 (Fig. 1e). The SAED pattern of the first-order dendrite branch is shown in Fig. 1f. The results obtained by interpreting of this SAED pattern showed that this is monoclinic modification of HfO_2. The zone axis of this crystal is directed along $[01\bar{1}\}]_m$.

The relative change of the density during crystallization of amorphous HfO_2 was analyzed using relation (2). Figure 2 shows the electron microscopy image of the HfO_2 film area before (a) and after (b) its complete crystallization. L_a and L_c are the distances between hardened Hf micro drops before and after film crystallization, respectively. The results of statistical treatment of measured relative density changes γ during the amorphous HfO_2 crystallization are shown in the form of frequency histograms in Fig. 2c. The γ distribution is characterized by the corrected root-mean-square deviation of 2.41 %, the positive asymmetry of 0.45, and the positive excess of 3.14. For comparison, Fig. 2c also shows the γ curve corresponding to the Gaussian distribution. At the reliability level of 0.5, the relative density change during hafnium dioxide film crystallization $\gamma = 2.51 \pm 1.66$ %. Hence, the growing microcrystal from the time of its nucleation and during growth is continuously subjected to tensile stresses from the side of the amorphous matrix, which can be a cause of one of the reasons for the development of the dendrite morphology of crystalline HfO_2.

The one-stage phase transformation in the amorphous film is accompanied by nucleation and growth of crystallite in the form of dendrites of the monoclinic modification of HfO_2, similar to dendrite 1 in Fig. 1a. The dependences of the average diameter D of the dendrites on time t for various growth rates are shown in Fig. 3a. Straight lines are constructed from the measurement data of D using the least squares method. The linear dependence $D(t)$ indicates on the constancy of the growth rate ν of each dendrite crystallite at a fixed electron current density through the sample. The value of ν

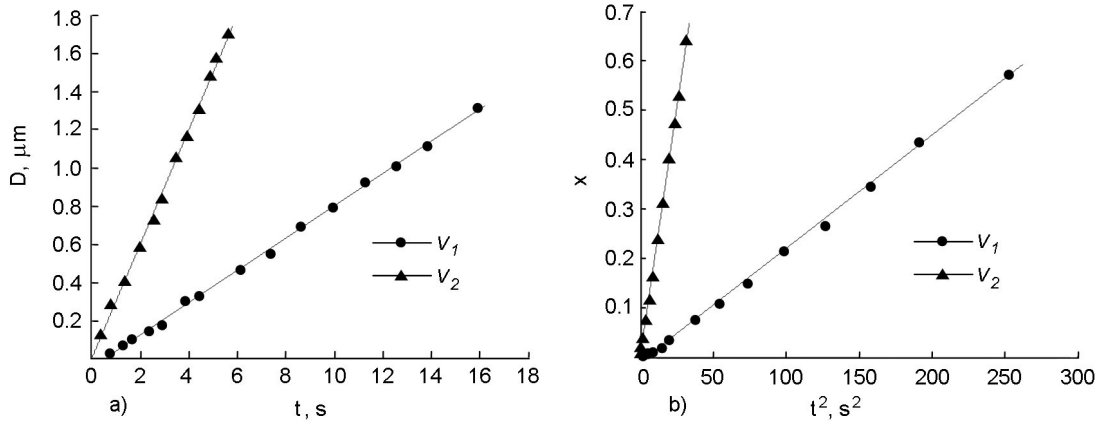

Fig. 3. Kinetics of single-stage crystallization of HfO_2. Dependences of the average diameter D of dendrites on time t (a) and dependences of the fraction of the crystalline phase x on t^2 (b) for various growth rates: $\nu_1 = 0.084$ μm·s^{-1}; $\nu_2 = 0.299$ μm·s^{-1}.

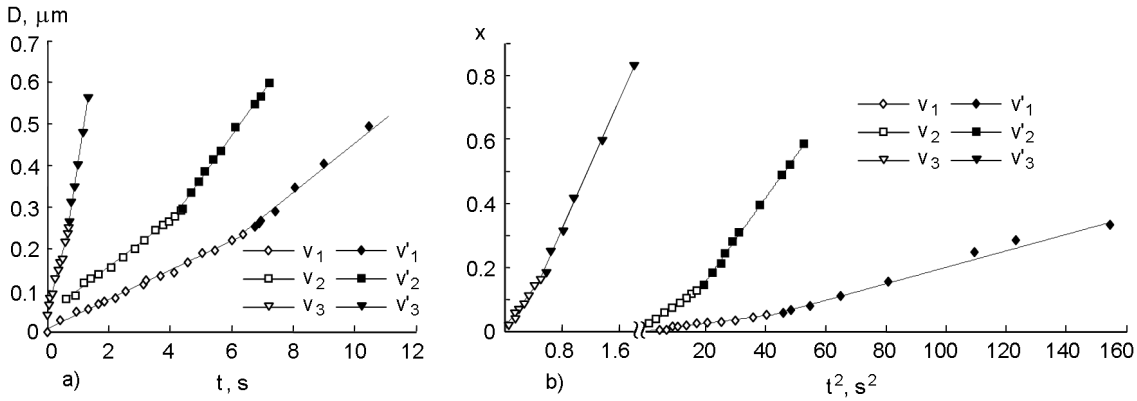

Fig. 4. Kinetics of two-stage crystallization of HfO_2. a) Dependences of the average diameter D of crystals on time t for various growth rates ν. b) Dependences of the crystalline phase fraction x on t^2. Growth rates of the crystals: $\nu_1 = 0.035$ μm·s^{-1}; $\nu_1' = 0.059$ μm·s^{-1}; $\nu_2 = 0.056$ μm·s^{-1}; $\nu_2' = 0.104$ μm·s^{-1}; $\nu_3 = 0.284$ μm·s^{-1}; $\nu_3' = 0.484$ μm·s^{-1}.

was determined from the slope of the straight line to the axis of abscissas: 0.084 μm·s^{-1}; $\nu_2 = 0.299$ μm·s^{-1}.

The kinetic curves of crystallization for the given values of ν are plotted in Fig. 3b. They reflects the dependence of the fraction of the crystalline phase x on time t, which has passed since the moment of the fixation of the onset of crystal formation. Since each crystal grew through the entire thickness of the film, the value of x was determined as the ratio of the area occupied by the crystal to the total area of the object area analyzed in the microscope. The kinetic curves in coordinates x — t^2 are straight lines. This indicates the quadratic dependence of x on t:

$$x = 0.002\, s^{-2} t^2 - 0.011, \qquad (4a)$$

$$x = 0.020\, s^{-2} t^2 + 3.3 \cdot 10^{-4}. \qquad (4b)$$

Expression (4a) corresponds to $\nu_1 = 0.084$ μm·s^{-1}, expression (4b) corresponds $\nu_2 = 0.299$ μm·s^{-1}.

The two-stage phase transformation in the amorphous film starts with the nucleation and growth of the disk-shaped crystals of orthorhombic modification of HfO_2 (crystals 2 in Fig. 1a and 1c). Then they split into domains with the orthorhombic and monoclinic modifications of HfO_2. This splitting takes place when the diameter D of disk-shaped crystals exceeds critical value of D^*. The dependences of the average diameter D of the crystals on time t for various growth rates are shown in Fig. 4a. While $D < D^*$, the disk-shaped crystals growth with a constant speed ν. After splitting, the growth rate of the crystals appreciably increases. If before splitting the

growth rate of the crystal is $\nu_1 = 0.035$ μm·s^{-1}, then after splitting its growth rate is $\nu_1' = 0.059$ μm·s^{-1}. Analogically $\nu_2 = 0.056$ μm·s^{-1} before splitting corresponds to $\nu_2' = 0.104$ μm·s^{-1} after splitting. And $\nu_3 = 0.284$ μm·s^{-1} before splitting corresponds to $\nu_3' = 0.484$ μm·s^{-1} after splitting (Fig. 4a).

The values of D^*, ν, and ν′, as well as the ratios ν′/ν for a series of crystallization sessions of amorphous hafnium dioxide are summarized in Table 1. According to the data in Table 1 after the crystal splitting its growth rate appreciably increases. There is no monotone dependence between D^* and ν, ν′ or ν′/ν. The results of statistical treatment of measured D^* are shown in the form of frequency f histogram in Fig. 5. The D^* distribution is characterized by the corrected root-mean-square deviation of 0.037 μm, the positive asymmetry of 0.57. At the reliability level of 0.5 the diameter value $D^* = 0.184 \pm 0.026$ μm.

The kinetic crystallization curves (Fig. 4b) in coordinates x — t^2 have the form of straight lines with a kink at the point t, corresponding to the moment, when $D = D^*$:

$$x = \alpha t^2 + \beta, \qquad (5a)$$

$$x = \alpha' t^2 + \beta'. \qquad (5b)$$

Expression (5a) describes the dependence of $x(t)$ for $D < D^*$. Expression (5b) describes the dependence of $x(t)$ for $D > D^*$. Numerical values of α, α′, β and β′ are given in Table 1.

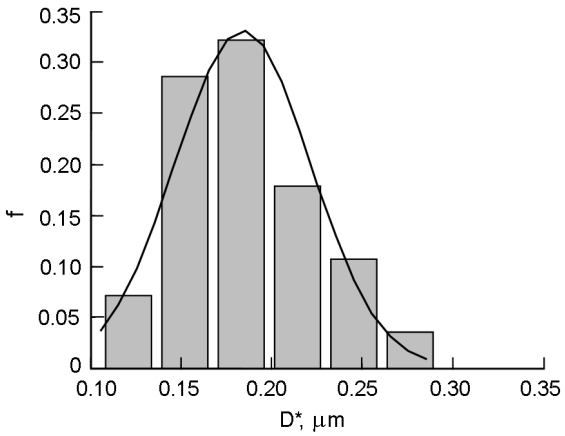

Fig. 5. Histogram of the relative frequencies f of the critical diameters D^* of HfO_2 crystals and the curve, corresponding to the Gaussian distribution.

The presence of the one-stage (amorphous phase-monoclinic phase of HfO_2) and the two-stage (amorphous phase-orthorhombic phase-monoclinic phase of HfO_2) transformations at electron beam irradiation of the amorphous film is due to the polymorphism of hafnium dioxide. At room temperature (and up to 1923 K), the monoclinic modification of HfO_2 is stable. This explains its dominant presence at the final stage of the film crystallization and the existence of a size — phase effect, when the HfO_2 crystal of the orthorhombic modification reaches the critical size (~ 0.2 μm) splits into domains with the monoclinic and orthorhombic crystal lattices. One of the vari-

Table 1. Parameters of a two-stage transformation during crystallization of amorphous film of HfO_2*

D^*, μm	0.143	0.160	0.235	0.266	0.294
ν, μm·s^{-1}	0.057	0.029	0.035	0.284	0.056
ν′, μm·s-1	0.244	0.036	0.059	0.4804	40.1
ν′/ν	4.28	1.24	1.69	1.70	1.86
α, s^{-2}	0.006	0.004	0.001	0.300	0.007
β	0.002	0.007	$0.3 \cdot 10^{-3}$	0.012	0.011
α′, s^{-2}	0.044	0.005	0.003	0.507	0.013
β′	-0.180	-0.015	-0.058	-0.088	-0.106

Notes. D^* is the critical diameter of the HfO_2 crystal at the moment of phase transformation from orthorhombic to monoclinic structure; ν is the growth rate of HfO_2 crystal before phase transformation; ν′ is the growth rate of HfO_2 crystal after phase transformation; α and β are the coefficients in the ratio (5a) before phase transformation; α′ and β′ are the coefficients in the ratio (5b) after phase transformation.

Table 2. The arithmetic means of characteristic unit of length <D0> and of relative length of crystallization <?0> for different types of polymorphic transformations of oxide films

Parameter	DPC of HfO_2 Laser evaporation (this work)	LPC of V_2O_3 Laser evaporation [16]	IPC of V_2O_3 Laser evaporation [16]	IPC of ZrO_2 Laser evaporation [15]	IPC of ZrO_2 Ion-plasma evaporation [15]
$<D_0>$	μm	1.59	2.24	0.68	0.46
$<\delta_0>$	3075	4553	1024	904	118

Notes. DPC – dendrite polymorphic crystallizations, LPC – layer polymorphic crystallizations, IPC – island polymorphic crystallizations.

ants of the conjugation of the orthorhombic and monoclinic lattices is given by (3).

According to the structural-morphological features, electron-beam crystallization of the amorphous hafnium dioxide corresponds to the dendrite polymorphic crystallization [12], when dendrite crystals are formed in the near-surface layer of the amorphous film with composition that corresponds to the composition of the amorphous film. Quantitative analysis of the features of the DPC of amorphous HfO_2 films is advisable to be carried out in a similar way as the analysis of LPC and IPC of amorphous V_2O_3 and ZrO_2 films [16]. By definition, a characteristic unit of time t_0 is the time, after which the volume of the amorphous phase decreases by a factor of e (wherein $x=1-e^{-1}=0.632$). The characteristic unit of length D_0 is the crystal size at time t_0 ($D_0 = \nu t_0$) [17].

At the one-stage crystallization of the film, according to (4a), the characteristic unit has length $D_{01} = 1.51$ μm, and according to (4b), the characteristic unit has length $D_{02} = 1.68$ μm. The values of D_{01} and D_{02} correspond to the crystal growth rates $\nu_1 = 0.084$ μm·s^{-1} and $\nu_2 = 0.299$ μm·s^{-1}. Their arithmetic mean $<D_0> = 1.59$ μm. Various branches of dendrites of HfO_2 have different crystallographic orientations. Therefore, the relative length of crystallization δ_0, introduced in [15, 16], should be defined as

$$\delta_0 = \frac{\langle D_0 \rangle}{\Omega^{1/3}}, \qquad (6)$$

where Ω is the volume of the unit cell of the monoclinic modification of HfO_2, equal to 138.28 Å^3 [18].

According to (6) for the dendrite polymorphic crystallization of HfO_2 the relative length of crystallization is $\delta_0 = 3075$. The arithmetic means $<D_0>$ and $<\delta_0>$ for different types of crystallization of HfO_2, V_2O_3 and ZrO_2 are given in Table 2. According to these data, the values of δ_0 for the DPC of HfO_2 and for the LPC of V_2O_3 are very close (several thousand). At the same time, there is a significant difference between the data, characterizing the dendrite polymorphous crystallization of HfO_2 and of its structural analogue ZrO_2 with island polymorphic crystallization, for which the value of δ_0 is several hundred.

The increasing of density of the film matter during crystallization of amorphous ZrO_2 is much higher than in the case of amorphous HfO_2. For ZrO_2 $\gamma = 10.27\pm2.14$ % [20], and for HfO_2 (present work) $\gamma = 2.51\pm1.66$ %. According to [5] with increasing temperature from the room temperature (amorphous HfO_2) to 750°C (crystalline HfO_2) the density of matter rises from 8.96 g·cm^{-3} to 9.40 g·cm^{-3}. For this case, according to (2), $\gamma = 4.91$ %, which is slightly higher than the upper limit of the confidence interval 4.17 %. For monoclinic phase of HfO_2 the density of matter is $\rho_c = 9.68$ g·cm^{-3} [19]. For the amorphous phase of HfO_2 the density of matter is $\rho_a = 9.39$ g·cm^{-3} [20]. In this case, according to (2), there is $\gamma = 3.09$ %. This value of γ falls within the confidence interval from 0.85 % to 4.17 %, that is established in this paper.

4. Conclusions

Amorphous films of HfO_2 were prepared with laser ablation of Hf in oxygen atmosphere at pressure of about 0.13 Pa on the substrates at the room temperature. Electron beam heating of the amorphous film initiates in it the dendrite polymorphic crystallization, which can be either single-stage or two-stage in nature. In the first

case, dendrites crystals of the monoclinic modification of HfO_2 are generated and grow at a constant tangential velocity. In the second case, at the initial stage, disc-shaped crystals of the orthorhombic modification of HfO_2 are growing. When their diameters exceed the critical value (~ 0.2 μm), the formation of domains with the monoclinic crystal lattice takes place in them. This is accompanied with a marked increasing in the growth rate and with the formation of the dendrite morphology. The crystallization kinetic parameters are determined and it is shown, that the quadratic dependence of the fraction of the crystalline phase on time is fulfilled. The average value of the relative length for the dendrite polymorphic crystallization is 3075. Crystallization of the amorphous HfO_2 is accompanied with densifying of the film material. The relative change in the density during its crystallization is about 2.5 %.

References

1. Nai-Wen Pi, Minghui Zhang, Jiechao Jiang et al., *Thin Solid Films*, **619**, 239 (2016).
2. Tsung-Ju Chen, Chin-Lung Kuo, *J. Appl. Phys*, **110**, 064105 (2011).
3. J.Lu, J.Aarik, J.Sundqvist et al., *J. Cryst. Growth*, **273**, 510 (2005).
4. Y.-S.Lin, R.Puthenkovilakam, J.P.Chang, *Appl. Phys. Lett.* **81**, 2041 (2002).
5. M.Modreanu, J.Sancho-Parramon, D.O'Connell et al., *Mater. Sci. Eng. B*, **118**, 127 (2005).
6. M.A.Pugachevskii, V.I.Panfilov, *Techn. Phys. Lett.*, **41**, 291 (2015).
7. A.G.Bagmut, I.A.Bagmut, V.A.Zhuchkov, M.O.Shevchenko, *Techn. Phys. Lett.* , **38**, 22 (2012).
8. A.G.Bagmut, I.A.Bagmut, V.A.Zhuchkov, M.O.Shevchenko, *Techn. Phys.*, **57**, 856 (2012).
9. B.J.Kooi, W.M.G.Groot, J.Th.M.De Hosson, *J. Appl. Phys.*, **95**, 924 (2004).
10. A.G.Bagmut, Electron Microscopy of Films Deposited by Laser Evaporation. Monograph, NTU "KhPI", Kharkiv (2014) [in Russian].
11. A.G.Bagmut, *Functional Materials*, **19**, 370 (2012).
12. A.G.Bagmut, *Techn. Phys. Lett.*, **38**, 488 (2012).
13. A.G.Bagmut, A.V.Taran, *J. Adv. Microsc. Res.*, **8**, 57 (2013).
14. A.G.Bagmut, S.N.Grigorov, V.Yu.Kolosov et al., *Functional Materials*, **10**, 687 (2003).
15. A.G.Bagmut, V.M.Beresnev, *Phys. Solid State*, **59**, 151 (2017).
16. A.G.Bagmut, *Phys. Solid State*, **59**, 1225 (2017).
17. A.N.Kolmogorov, *Izv. Akad. Nauk SSSR*, **3**, 355 (1937).
18. JCPDS Powder Diffraction File Card No. 43-1017 (International Centre for Diffraction Data, Swarthmore, PA, 1996).
19. S.V.Ushakov, A.Navrotsky, Y.Yang et al., *Phys. Stat. Solidi (b)*, **241**, 2268 (2004).
20. D.Ceresoli, D.Vanderbilt, *Phys. Rev. B*, **74**, 125108 (2006).